

2-D Anticlinal Structure Modeling Using Feed-Forward Neural Network (FNN) Inversion of Profile Gravity Data: A Case Study from Iran

Eshaghzadeh, A.^{1*}, Seyedi Sahebari, S.² and Kalantari, R. S.³

1. Ph.D. Student, Department of Geology, Faculty of Sciences, University of Isfahan, Isfahan, Iran

2. Instructor, Department of civil Engineering, University College of Nabi Akram, Tabriz, Iran

3. M.Sc. Graduated, Department of Earth Physics, Institute of Geophysics, University of Tehran, Tehran, Iran

(Received: 27 Aug 2019, Accepted: 24 Jan 2021)

Abstract

The Anticlines are the main hydrocarbon traps on land or at sea. This structure is considered as the target of the many projects of gravity exploration all over the world. Artificial neural networks (ANNs) are used in order to solve prediction, estimation, and optimization problems. In this paper, the feed-forward neural network (FNN) is applied for modeling the anticlinal structure using gravity anomaly profile and the back propagation algorithm is used for artificial neural network training. Moreover, the scalene triangle model is employed to describe the geometry of anticlinal structure in analyzing gravity anomalies. In terms of neural network training, eight features among the synthetic gravity field variations curves along 22500 profiles are defined. These gravity profiles are computed based on different values of the scalene triangle parameters consisting of the top depth, bottom depth, limb angles and density contrast. The defined neural network contain three layers, eight neurons (the number of features) in the input layer, 30 neurons in the hidden layer and six neurons (the number of scalene triangle parameters) in the output layer. In order to evaluate the performance of the trained neural network, the specified features related to a synthetic model, with and without random noise, are applied as the input data to train neural network. The parameters estimation error by FNN is negligible. The proposed method is illustrated with a real gravity data set from Korand region, Iran. The inferred anticlinal structures are compared with the interpreted map of the seismic data.

Keywords: Anticlinal structure, Feed-forward neural network (FNN), Gravity, Scalene triangle, Iran.

1. Introduction

Anticlines are amongst the most important geological structures in regional studies and hydrocarbon exploration using potential methods. In general, inversion of gravity anomalies is non-unique in the sense that the observed gravity anomalies in a survey can be explained by a variety of density distributions. To resolve such ambiguity, the anomalous mass should be estimated by a suitable geometry with a defined density contrast. Several forward gravity modeling schemes have been proposed based on constant or variable density contrast for anticlinal structure (Rao and Avasthi, 1973; Heiland, 1968; Rao and Murty, 1978; Chakravarthi and Sundararajan, 2007 and 2008). Although the exhibited methods differ in the definition of the density changes in proportion to depth, the normal isosceles triangular model is generally used to describe the geometry of this structure to analyze gravity anomalies (Chakravarthi and Sundararajan, 2007). Since the anticlinal structures in nature have mostly two non-

isocline flank, utilization of the isosceles triangular model will be accompanied by a large error in the modeling. Using the scalene triangle so as to reducing errors has been proposed. In this study, the density contrast has been assumed constant with depth.

Artificial neural networks (ANNs) aim at modeling using the information processing by nervous systems. Their application to solve a wide range of problems in various scientific fields makes them very distinctive. The ANNs are useful and powerful tools for analyzing automatically and consequently presenting sagacious interpretation of the gravity field data. In this paper, a new method for anticline structure modeling based on feed-forward neural network (FNN) is presented. The network has been trained by the features extracted from a set of synthetic data and the model parameters as input and output. Back propagation algorithm is used in order to train the FNN. The back propagation is defined as an approximate steepest descent algorithm that minimizes mean square error.

*Corresponding author:

eshaghzadeh.ata@gmail.com

ANNs can be a vigorous and smart implement for performing nonlinear functional mapping between a set of input variables such as gravity field data and a set of output or source parameters, together with particular procedures for optimizing the mapping (Bishop and Hinton, 1995). Neural networks (NNs) have been employed for interpreting well logs (Huang et al., 1996), recognizing seismic wave forms (Ashida, 1996) and automatic detection of buried utilities and solid objects from GPR data (Al-Nuaimy et al., 2000). In addition, ANNs are frequently employed for the potential data interpretation. For example, the back propagation network was used for structural interpretation of aeromagnetic data (Pearson et al., 1990), classification of buried objects from their magnetic signatures (Brown, et al., 1996) and detection of tunnels from gravity data (Salem et al., 2001). Depth and radius of subsurface cavities are determined from microgravity data using back propagation neural network (Eslam et al., 2001). The forced neural network was used by Osman et al. (2006) to interpret a profile of the residual gravity anomaly and, consequently, by Osman et al. (2007) to provide a forward modeling for gravity anomaly profile. Al-Garni (2013) used the modular neural network (MNN) inversion to compute the depth and the shape factor of the causative target from a gravity anomaly. Eshaghzadeh and Hajian (2018) introduced a new concept of the modularity for analysis of the gravity field by modular neural network. The feed forward neural networks have been tested for the synthetic gravity data, with and without noise. The results indicate that FNNs, if trained adequately, are able to evaluate the scalene triangle parameters correctly. The proposed technique is applied to gravity data from Korand region in north of Iran to estimate the parameters of the anticlinal structure. The results demonstrate high similarity with the results attained from seismic operation.

2. Forward Gravity Modeling of Scalene Triangle

For FNN training, we need to determine a series of features from the calculated gravity field of a scalene triangle model. Figure 1 displays a schematic view of 2D geometry of

anticlinal structure. The Z-axis is positive downward and the X-axis is transverse to the strike of the model. While, z_1 and z_2 are the depths to the top and bottom of the model and i and j are the angles of the anticline limb as shown in Figure 1. It is worth mentioning that the gravity anomaly $\Delta g(x)$ at any point $P(x',0)$ on the X-axis can be derived from the fundamental equation of a gravity anomaly due to a 2D source with a cross-sectional area s (Rao and Murthy, 1978):

$$\Delta g(x) = 2G \int_S \frac{\Delta \rho z dv dz}{r^2} \quad (1)$$

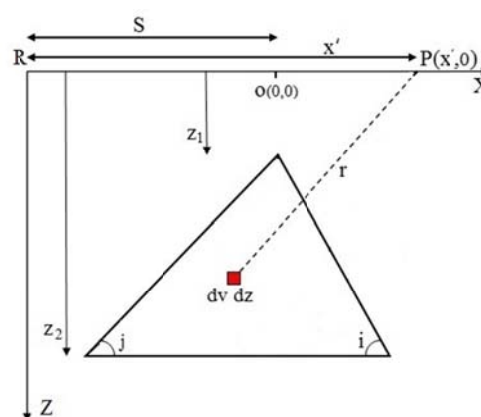


Figure 1. Geometry of anticlinal structure.

where G is the universal gravitational constant, $dv dz$ is the cross-sectional area of a linear mass, $\Delta \rho$ is the density contrast between an anticlinal structure and its covering sediments, and r is the radial distance from the element $dv dz$ to the point $P(x',0)$. Substituting limits for spatial coordinates, the gravity anomaly of anticlinal structure on the main profile can be expressed from Figure 1 as:

$$\Delta g(x) = 2G \int_{z=z_1}^{z_2} \int_{v=-(z-z_1)\cot j}^{(z-z_1)\cot i} \frac{\Delta \rho z dv dz}{z^2 + (v-x)^2} \quad (2)$$

where $x=x'-S$, S is the distance of the origin of the model from the reference point, R (Figure 1). On integration, Equation (2) can be rewritten as:

$$\Delta g(x) = 2G \Delta \rho \left\{ \frac{[(A-B) - (C-D)] - [(E-F) - (H-I)]}{\dots} \right\} \quad (3)$$

where

$$A = -z_2 \tan^{-1} \left(\frac{x - (z_2 - z_1) \cot(i)}{z_2} \right) \quad (4)$$

$$B = \left\{ \left\langle \left((x + z_1 \cot(i)) \left[\ln \left(\frac{z_1^2 \cos(2i)}{2} - \frac{x^2 \cos(2i)}{2} - z_2 z_1 + \frac{x^2}{2} + z_2^2 + \frac{z_1^2}{2} - z_2 z_1 \cos(2i) - x z_2 \sin(2i) + x z_1 \sin(2i) \right) - 2 \cot(i) \tan^{-1} \left(\frac{z_1 \cot^2(i) + x \cot(i)}{x + z_1 \cot(i)} - \frac{z_2 (2 \cot^2(i) + 2)}{2(x + z_1 \cot(i))} \right) \right] \right\rangle \times \frac{1}{2 \cot^2(i) + 1} \right\} \quad (5)$$

$$C = -z_1 \tan^{-1} \frac{x}{z_1} \quad (6)$$

$$D = \left\{ \left\langle \left((x + z_1 \cot(i)) \left[\ln \left(\frac{z_1^2 \cos(2i)}{2} - \frac{x^2 \cos(2i)}{2} + \frac{x^2}{2} + \frac{z_1^2}{2} - z_1^2 \cos(2i) - x z_1 \sin(2i) + x z_1 \sin(2i) - 2 \cot(i) \tan^{-1} \left(\frac{z_1 \cot^2(i) + x \cot(i)}{x + z_1 \cot(i)} - \frac{z_1 (2 \cot^2(i) + 2)}{2(x + z_1 \cot(i))} \right) \right] \right\rangle \times \frac{1}{2 \cot^2(i) + 1} \right\} \quad (7)$$

$$E = -z_2 \tan^{-1} \left(\frac{x + (z_2 - z_1) \cot(i)}{z_2} \right) \quad (8)$$

$$F = \left\{ \left\langle \left((x - z_1 \cot(j)) \left[\ln \left(\frac{z_1^2 \cos(2j)}{2} - \frac{x^2 \cos(2j)}{2} - z_2 z_1 + \frac{x^2}{2} + z_2^2 + \frac{z_1^2}{2} - z_2 z_1 \cos(2j) + x z_2 \sin(2j) - x z_1 \sin(2j) \right) + 2 \cot(j) \tan^{-1} \left(\frac{z_1 \cot^2(j) - x \cot(j)}{x - z_1 \cot(j)} - \frac{z_2 (2 \cot^2(j) + 2)}{2(x - z_1 \cot(j))} \right) \right] \right\rangle \times \frac{1}{2 \cot^2(j) + 1} \right\} \quad (9)$$

$$H = -z_1 \tan^{-1} \frac{x}{z_1} \quad (10)$$

$$I = \left\{ \left\langle \left((x - z_1 \cot(j)) \left[\ln \left(\frac{z_1^2 \cos(2j)}{2} - \frac{x^2 \cos(2j)}{2} + \frac{x^2}{2} + \frac{z_1^2}{2} - z_1^2 \cos(2j) + x z_1 \sin(2j) - x z_1 \sin(2j) \right) + 2 \cot(j) \tan^{-1} \left(\frac{z_1 \cot^2(j) - x \cot(j)}{x - z_1 \cot(j)} - \frac{z_1 (2 \cot^2(j) + 2)}{2(x - z_1 \cot(j))} \right) \right] \right\rangle \times \frac{1}{2 \cot^2(j) + 1} \right\} \quad (11)$$

3. Feed-Forward Neural Network (FNN)

Today, the FNN is regarded as an important neural network. The case of non-linear problems consists of at least three layers. As seen, a schematic diagram of a FNN is shown in Figure 2, where information flows from inputs to outputs in only one direction. The leftmost layer in this network is called the input layer, and the neurons or processing elements within the layer are named the input neurons. The network takes the data through this layer. Each neuron consists of a vector of modifiable weights or connection strengths

(Macias et al., 2000). The rightmost or output layer contains the output neurons, as in this case, there is a single output neuron. The output neuron or neurons have distinct sets of weights and process the input values to generate a result (El-Kaliouby and Al-Garni, 2009). The middle layer is called a hidden layer which can contain the different numbers of processing elements. Each neuron transmits a single data value over weighted connection to the hidden neurons where they process the input data and dispatch their results to the output layer.

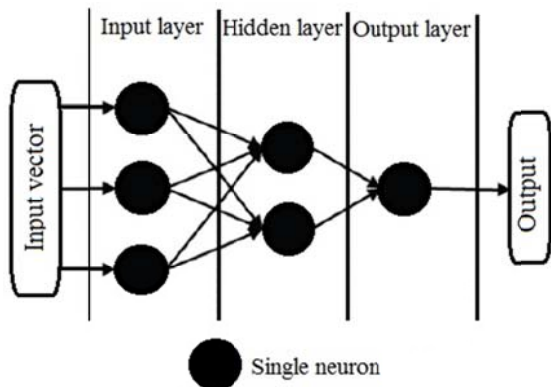


Figure 2. Feed-forward topology of an artificial neural network.

In this paper, FNN is used for estimating the model parameters estimation by the specified features from the gravity forward modeling of the scalene triangle model. As for the FNN to recognize the pattern of the gravity profile data, some features are defined as the input of the FNN. For neural network learning with gravity data, some features are selected from the profile of the gravity field undulation. In other words, there must be a relation with the geometrical parameters of the anticline. We can divide the process of the NN procedure into three parts: the first, training data production (in such cases study using

forward modeling), the second, neural network training and the third part, NN inverse modeling.

4. Neural Network Training

ANNs can be categorized into two main categories: unsupervised recurrent and supervised feed-forward networks. In the unsupervised recurrent type, the networks allow information to flow in both directions. These models are called unsupervised given the fact that there was no supervision on the set-out of the input-output mapping relation during the learning phase. On the other hand, in the supervised model, through a set of correct input-output pairs called the training set, the network learns the relation between the input-output pairs which has been used in the back propagation algorithm for network training. As a matter of fact, the aim of neural network training is to construct a relationship between known input-output parameters for a given problem to apply the trained network to input parameters with unknown outputs later on. Figure 3 depicts the gravity field variations along a profile for the 2D scalene triangle model with the parameters $z_1=1$ km, $z_2=4$ km, $i=40^\circ$, $j=20^\circ$ and $\Delta\rho=100$ kg/m³.

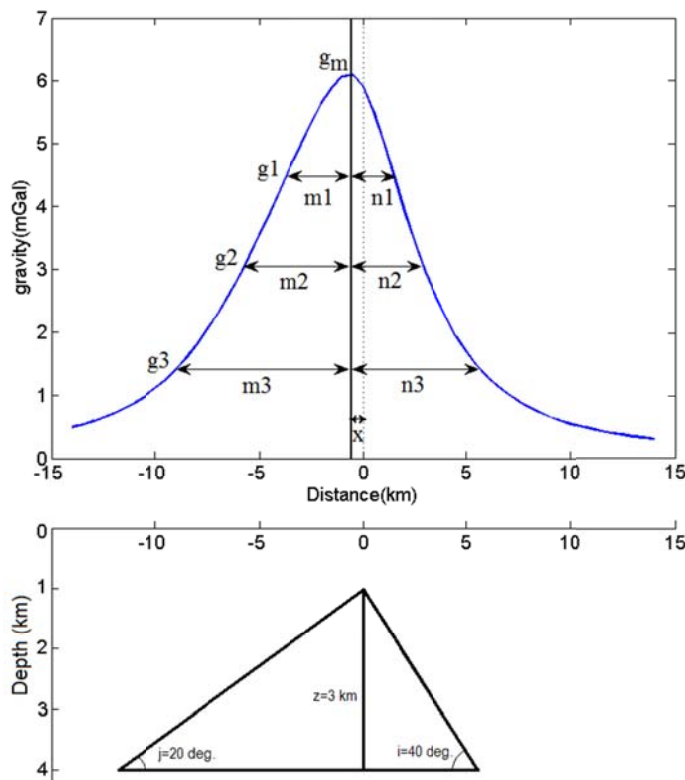


Figure 3. A pattern for estimating features from the gravity anomaly curve (upper) of an anticlinal structure (below).

Considering Figure 3 as a criterion, the features are defined as following:

f1= maximum gravity, g_m .

f2= ratio of n_1 to m_1 in g_1 where the gravity value is 75% of the maximum gravity value.

f3= ratio of n_2 to m_2 in g_2 where the gravity value is 50% of the maximum gravity.

f4= ratio of n_3 to m_3 in g_3 point where the gravity value is 25% of the maximum gravity.

f5= ratio of width of curve in g_3 to the width of curve in g_2 , $(n_3+m_3)/(n_2+m_2)$.

f6= ratio of the width of curve in g_3 point to the width of curve in g_1 point, $(n_3+m_3)/(n_1+m_1)$.

f7= ratio of the gravity values difference in g_m and g_2 points to the gravity values difference in g_1 and g_3 points, $(g_m-g_2)/(g_1-g_3)$.

f8= horizontal distance between the origin to maximum gravity (x in Figure 3).

Since there are eight defined features, input layer in neural network includes eight neurons. The outputs are geometric characteristics related to the anticlinal structure, namely z_1 , z_2 , i , j , $\Delta\rho$ and x . Hence, the output layer of the neural network contains six neurons. The correct number of hidden neurons can be determined more reliably by trial-and-error methods. Here, 30 neurons have been applied in the hidden layer. Figure 4 reveals the structure of FNN used for the gravity inverse modeling in this paper.

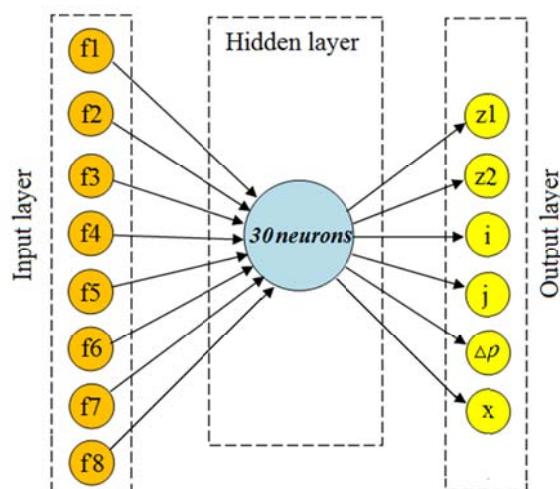


Figure 4. The structure of the designed three-layers FNN with eight neurons in the input layer, 30 neurons in the hidden layer and six neurons in the output layer.

In order to propose a method to estimate the geometric parameters of the anticlinal structure, the trained neural network is required. The gravity effect of the scalene triangle model has been calculated to measure the limits of the parameters z_1 , z_2 , $\Delta\rho$ as well as angles i and j , respectively, from 3 to 4.5 km with five points in this range, from 4.5 to 6 km with five points in this range, from 100 to 400 kg/m^3 with six points in this range, from 15 to 40 degree with six points in this range. The parameter x related to each forward modeling is computed separately, as for horizontal distance is considered five points between 0 to 1 km. The point of note is that the values of the parameters have been selected randomly for each forward modeling. Therefore, 180000 features are extracted from 22500 estimated gravity profiles. The parameters ranges have been chosen based on the action of measured gravity field data and the geological information of the study region. Afterwards, the defined features relevant to each gravity field variations curves are obtained as training data or patterns. The most widely used training method is known as the back propagation method. The back propagation method produces a least-square fit between the actual network output and a desired output by computing a local gradient in terms of the network weights (Rummelhart *et al.*, 1986). The weighted sum of the inputs is rescaled by an activation function before transferring to the hidden layer and also the weighted sum of the hidden layer neurons is rescaled by means of an activation function before transferring to the output layer. The sigmoid function has been employed for the first layer and the linear activation function for the output layer (Figure 5).


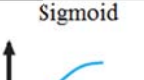
Activation function	Comments
 Linear	Perfect storage of any pattern, but amplifies noise.
 Sigmoid	Suppresses noise, contrast enhances, not quantized.

Figure 5. Specifications of the linear and sigmoid activation function (Rojas, 1996).

The sigmoid function is one of the most popular activation functions for back propagation networks. A symmetrical activation function has some advantages for FNN learning. The symmetrical sigmoid is defined as (Rojas, 1996):

$$S_s(x) = \frac{1 - e^{-x}}{1 + e^{-x}} \quad (12)$$

This method requires computation of the gradient of the error function at each iteration step. The amount of the error is given by (Macias et al., 2000)

$$E = \frac{1}{2} \sum_{l=1}^N \sum_{k=1}^M (y_k^l - o_k^l)^2 \quad (13)$$

Here, N is the numbers of input vector, M is the numbers of the model parameters, y is the model parameters and o is the resulted model parameters by the FNN. Back propagation solves the problem directly by minimizing E . To train the NN, 70% of the pattern has been

employed. Furthermore, 15% of the patterns are used for the final NN testing and analysis and the remaining 15% of patterns are utilized for the validation to prevent the overfitting. Figure 6 indicates the mean squared error variations of the NN training, testing and validation versus the iteration increase. The training set is used to compute gradients to determine the weight update at each iteration. When the validation error grows for a specified number of iterations, the training is stopped, and the weights causing the minimum error on the validation set are used as the final trained network weights (Hagan et al., 1996). In Figure 6, the goal is the defined minimum error, that is 0.1 and the best is the computed minimum error that is 0.885 at iteration 87. The histogram of errors has been exhibited in Figure 7. The y -axis represents the number of errors that falls within each interval on the x -axis. Based on the results of the error analysis, the process of the NN training was well accomplished.

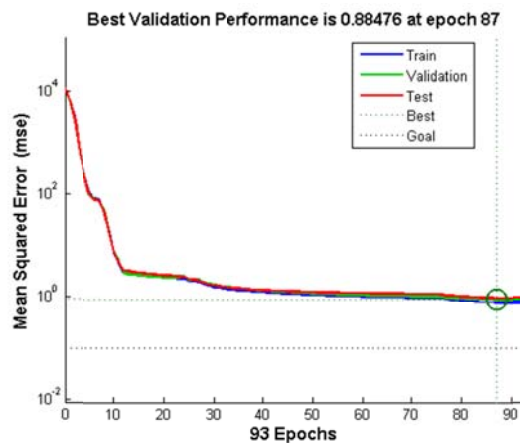


Figure 6. Mean squared error reduction versus iteration for achieving a trained FNN.

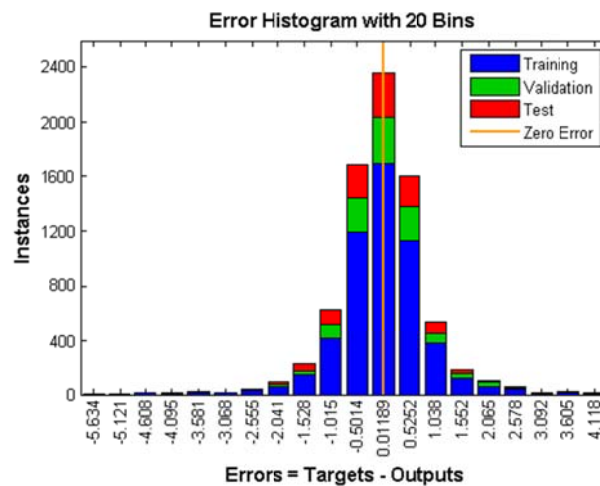


Figure 7. The histogram of mean squared error.

5. Synthetic Gravity Data Inverse Modeling

The drawn curve in red in Figure 8 demonstrates the theoretical noise-free gravity anomaly of a scalene triangle model while the parameters assumed for this model are $z_1=3$ km, $z_2=5$ km, $i=20^\circ$, $j=30^\circ$ and $\Delta\rho=150$ kg/m³. The sampling is performed at 57 points along a 28 km profile with 0.5 km interval. The gravity response of the resulted parameters with the FNN inverse modeling for noise-free data has been displayed in Figure 8 by the black curve. To check the trained FNN performance in the existence of noise for estimating the parameters of the gravity anomaly causative target, two sets of random noise with different amplitudes added to the synthetic gravity anomaly data by following equations:

$$g_{noise}(x_i) = g(x_i) + 0.2(\text{RAN}(i) - 0.5) \quad (14)$$

$$g_{noise}(x_i) = g(x_i) + 0.5(\text{RAN}(i) - 0.5) \quad (15)$$

where $g_{noise}(x_i)$ is the noisy gravity anomaly value at x_i and $\text{RND}(i)$ is a pseudo-random number whose range is (0, 1).

The red curves in Figures 9 and 10 represent the corrupted data by two random noise set with an amplitude of 0.2 mGal and 0.5 mGal, respectively. The generated gravity of the inferred structures with the FNN inverse modeling for noisy synthetic gravity data have been displayed in Figures 9 and 10 by the black curves.

In order to quantitative comparison, the errors between the forward modeling gravity or observed gravity and the estimated gravity from the FNN output are calculated using the root mean square error (RMSE) (Asfahani and Tlas, 2008):

$$RMSE = \sqrt{\frac{1}{N} \sum_{i=1}^N [(g_i^{obs} - g_i^{FNN})^2]} \quad (16)$$

where g^{obs} is the observed or modeled gravity, g^{FNN} is the rated gravity by FNN and N is the number of gravity data set.

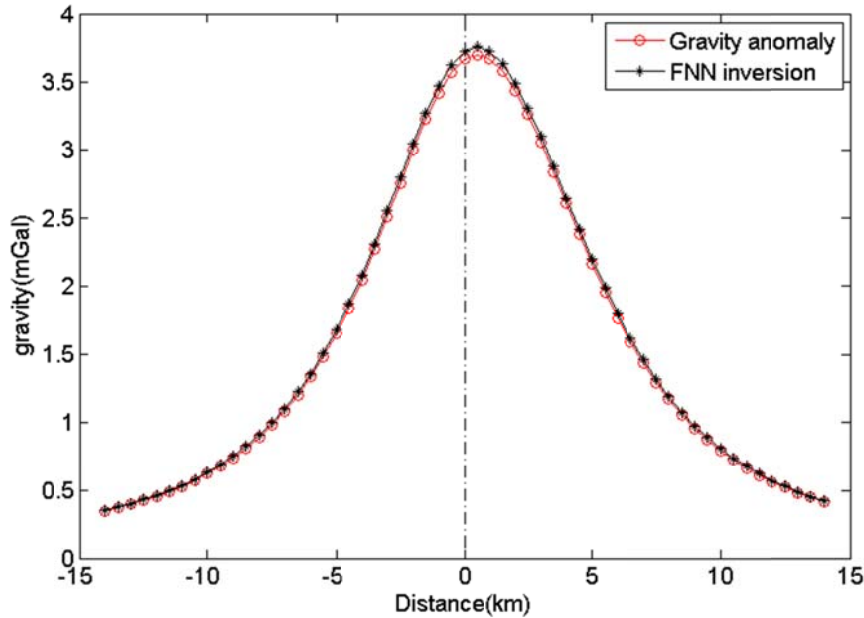


Figure 8. The free-noise gravity field data of the scalene triangle synthetic model with parameters $z_1=3$ km, $z_2=5$ km, $i=20^\circ$, $j=30^\circ$ and $\Delta\rho=150$ kg/m³ (red curve), and the gravity responses of the FNN inversion (black curve).

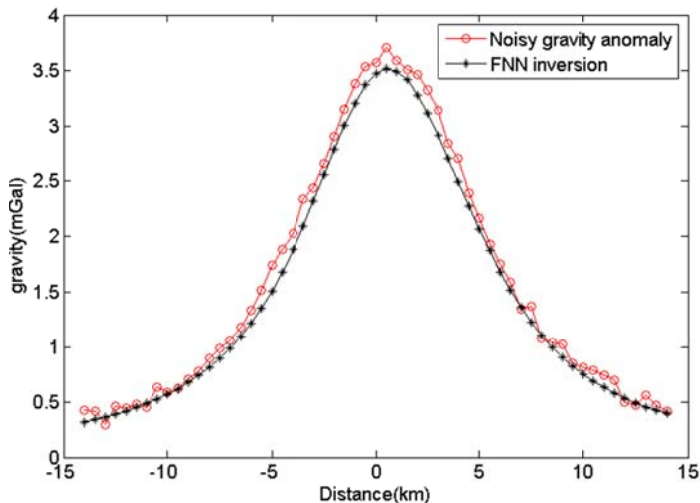


Figure 9. The black curve shows the gravity response of the FNN inverse modeling for the theoretical gravity data imposed by a random noise of 0.2 mGal amplitude (red curve).

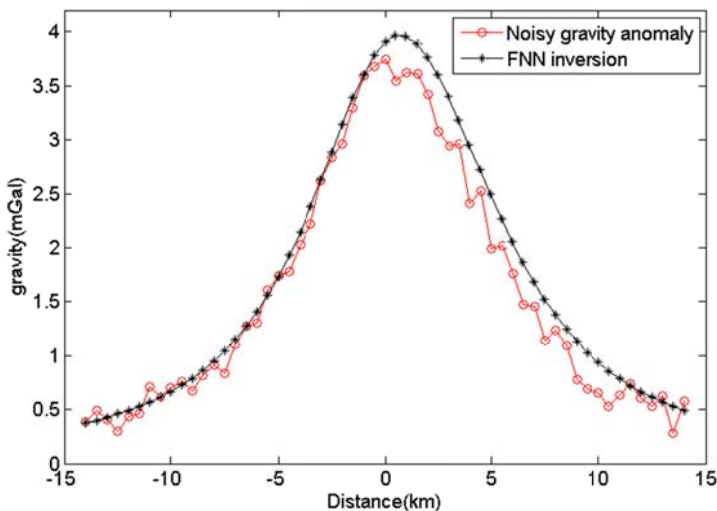


Figure 10. The black curve shows the gravity response of the FNN inverse modeling for the theoretical gravity data imposed by a random noise of 0.5 mGal amplitude (red curve).

The numerical results of the FNN inverse modeling for the synthetic data, with and without noise, and evaluated errors have been given in Table 1. The errors in the

estimation of the depths, angles and density contrast increase proportionally with the noise ratio. The results are satisfactory and acceptable.

Table 1. The initial parameters of the scalene triangle synthetic model and estimated parameters using FNN inversion.

	Parameters						
	Z1 (km)	Z2 (km)	I (deg)	J (deg)	$\Delta\rho$ (kg/m ³)	x (km)	RMSE
Initial values	3	5	20	30	150		
Free-noise gravity data	2.98	5.01	20.13	30	148.7	0.5	0.025
Error %	0.7	0.3	0.65	0	0.87	0.5	
With a noise of 2 mGal amplitude	3.05	4.95	19.36	31.62	156.4	0.494	0.187
Error %	1.7	1	3.2	5.4	4.3	1.2	
With a noise of 5 mGal amplitude	3.09	5.12	18.57	32.27	158.1	0.487	0.237
Error %	3	2.4	7.15	7.6	5.4	2.6	

6. Field Example

The region under study named Korand is located in Golestan province, northeastern Iran. The yellow cursor on the rightmost side picture in Figure 11 displays the position of Korand region. As evident, the region lies in the Kopet Dagh geological and structural unit covered by the quaternary thick sediments. Figure 12 displays the geological map of the study region. The blue rectangular on the geological map shows the gravity field measurement area limits. Because of the hydrocarbon reservoirs, this zone is important and noteworthy. The aim of the gravity

observation is to detect the anticline as the hydrocarbon trap.

Figures 13 and 14 present the contour map related to the Bouguer gravity anomaly and the topography map of the area under consideration, correspondingly. The altitudinal map depicts the height reduction from the southeast to the northwest, gradually. Removing a quadratic trend from the Bouguer anomaly map, the residual gravity anomaly relevant to the exploration region is computed (Figure 15). The positive anomaly noticeable in the residual gravity map center is related to an antiformal structure.

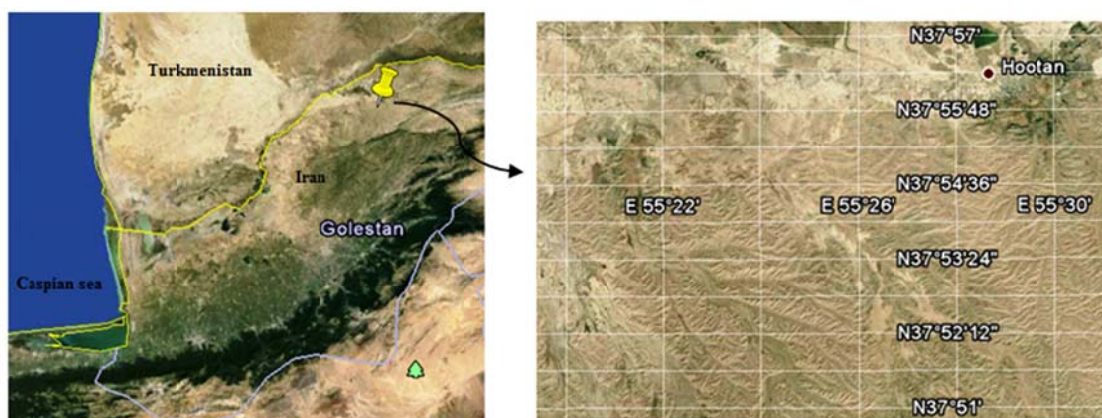


Figure 11. The satellite image of the area under consideration, namely Korand (yellow cursor in left-hand side picture). The rightmost side picture shows the morphology of Korand.

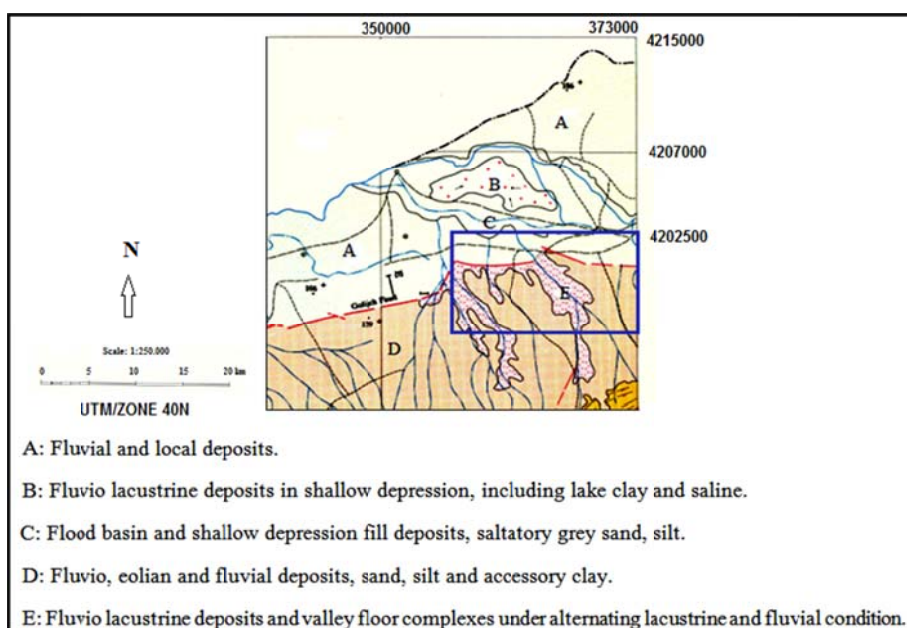


Figure 12. The geological map of Korand. The blue rectangular displays the study area limits.

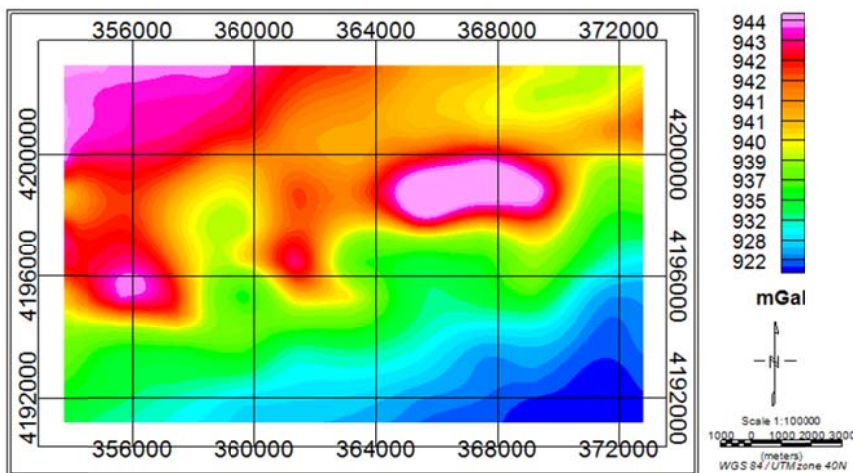


Figure 13. The contour map of the Bouguer gravity field.

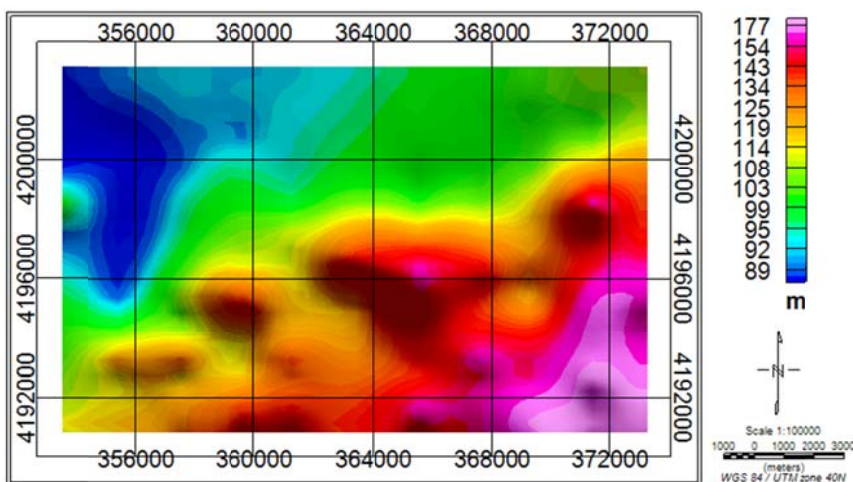


Figure 14. The topography map of Korand area.

The data were picked up at 100 m interval along Profiles A-A', B-B' and C-C' in the gravity anomaly for inverse modeling using FNN; the gravity field variations along these profiles as well as the results of the FNN inversion responses has been revealed in

Figures 16, 17 and 18, separately. The inverted parameters using FNN and error estimates are tabulated in Table 2. The x_0 in Table 2 shows the evaluated position of the ridge of the subsurface inferred anticlinal structure.

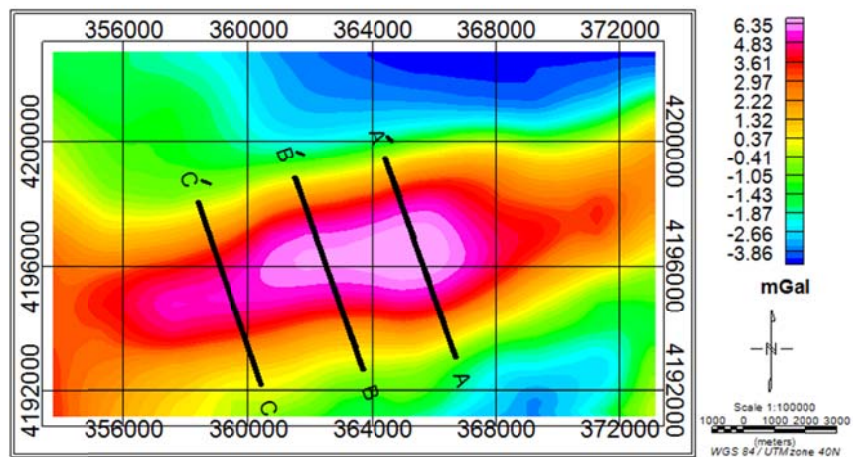


Figure 15. The residual gravity anomaly map. The direction of the profiles A-A', B-B' and C-C' has been presented in map.

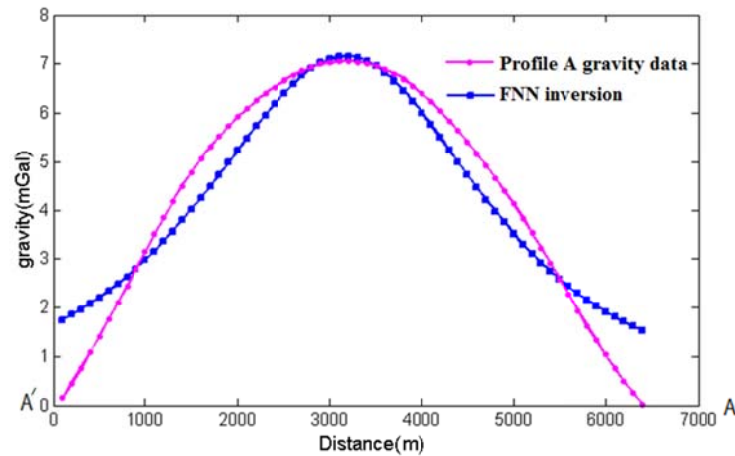


Figure 16. The gravity field variations along profile A-A' and the gravity response of the inverted parameters by FNN.

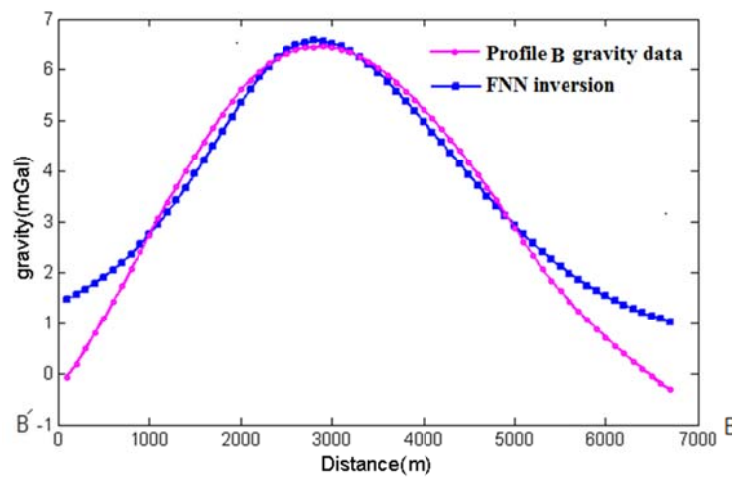


Figure 17. The gravity field variations along profile B-B' and the gravity response of the inverted parameters by FNN.

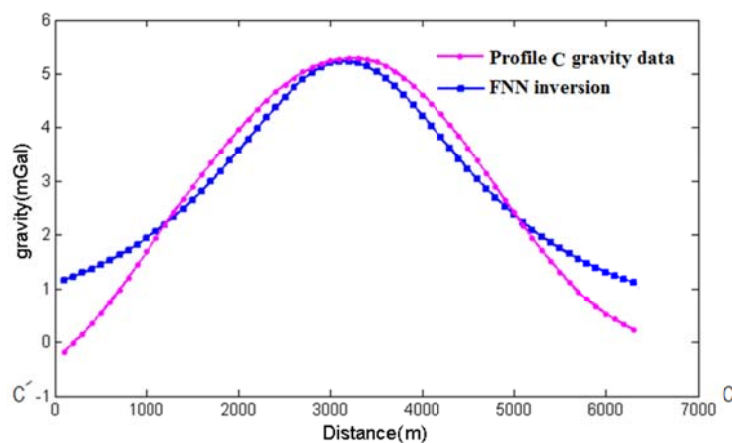


Figure 18. The gravity field variations along profile C-C' and the gravity response of the inverted parameters by FNN.

Table 2. Evaluated parameters using the FNN inversion for the profiles A-A', B-B' and C-C'.

Profile	Parameters						
	Z1 (km)	Z2 (km)	I (deg.)	J (deg.)	$\Delta\rho$ (kg/m ³)	x_0 (km)	RMSE
A-A'	3.43	5.16	24.93	21.36	372.8	3.5	0.741
B-B'	3.65	5.34	33.1	18.04	383.4	3.6	0.264
C-C'	3.86	5.37	26.2	25.85	391.7	3.4	0.502

In Korand area, the Tirgan formation found the upper surface of the anticline because of its solidity and hardness against erosion. The depth contour map of the anticlinal structure based on the seismic data analysis (Figure 19) demonstrate which one of the determined depths parameters using FNN inversion have a good conformity with the estimated ones in the seismic approach.

7. Discussion and Conclusion

The presence of error in the geophysical modeling and numerical computation is unavoidable due to some factors such as the heterogeneity and discontinuity of the interior geological structures, the incoherence and incompatibility of the undersurface structures, and masses configuration with geometric shapes. Therefore, the proposed method, which is FNN, is not an exception as well. In another word, the existence of error in FNN inversion response is unavoidable.

In this paper, an innovative approach has been developed based on the FNN with three layers to determine the top and bottom depth, angles and density contrast parameters of an anticlinal structure from gravity anomaly data. We have characterized the antiformal formation analogous the scalene triangle model, geometrically. Moreover, a new method has been presented for computing the

profile gravity data of an anticlinal structure with various slopes.

Geological information plays an important role in the training data production. We have used a data set with 180000 features extracted from the gravity forward modeling for training and testing the neural network. The designed network was tested by both synthetic and real gravity data. The validity of this method was tested using noise-free and noise-corrupted synthetic models, from which the satisfactory results obtained. The results of error analysis demonstrate that the FNN is sensitive to the noise, as the root mean square error estimates for the free-noise data and the added noise of 0.2 mGal and 0.5 mGal amplitudes to the synthetic data are 0.025, 0.187 and 0.237, respectively.

We have compared the inverted depths parameters using FNN with the ones estimated by the seismic method. The FNN inverse modeling results confirm well to the seismic data interpretation. The numerical results of both methods show that the depth follows an upward trend from east to west, but the maximum depth estimation shows significant differences. The average of the density contrast in the field has been computed as 382.6 kg/m^3 . We can conclude that the FNN is a powerful, intelligent and exact method for the gravity data modeling and resolution.

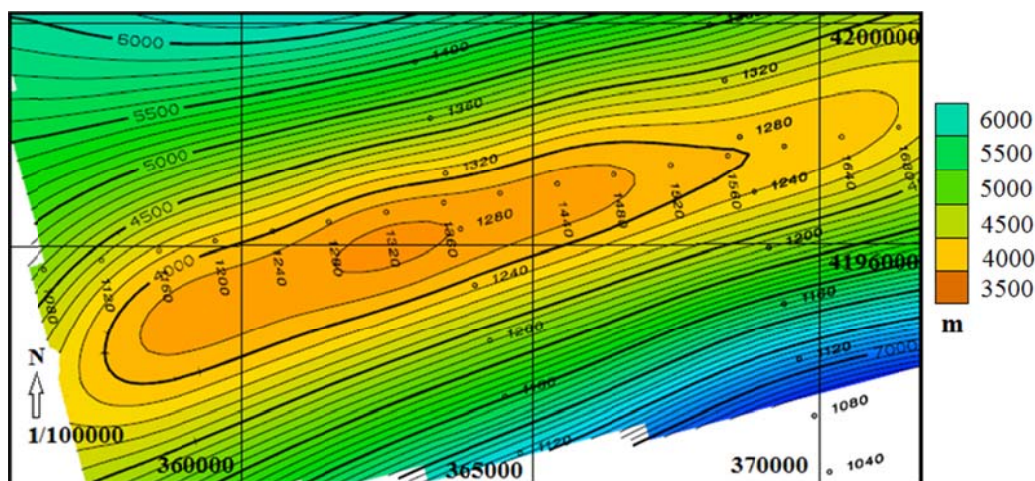


Figure 19. The depth contour map extracted from the seismic data for the Tirgan horizon.

References

- Al-Garni, M.A., 2013, Inversion of residual gravity anomalies using neural network. *Arab J. Geosci.*, 6, 1509–1516.
- Al-Nuaimy, W., Huang, Y., Nakhkash, M. and Eriksen, A., 2000, Automatic detection of buried utilities and solid objects with GPR using neural networks and pattern recognition. *Journal of Applied Geophysics*, 43, 157-165.
- Asfahani, J. and Tlas, M., 2008, An automatic method of direct interpretation of residual gravity anomaly profiles due to spheres and cylinders. *Pure Appl. Geophys.*, 165, 981-994.
- Ashida, Y., 1996, Data processing of reflection seismic data by use of neural network. *Journal of Applied Geophysics*, 35, 89-98.
- Bishop, C.M. and Hinton, G., 1995, *Neural Networks for Pattern Recognition*. Clarendon Press, Oxford.
- Brown, M.P. and Poulton, M.M., 1996, Locating buried objects for environmental site investigations using Neural Networks. *JEEG*, 1, 179-188.
- Chakravarthi, V. and Sundararajan, N., 2007, Marquardt optimization of gravity anomalies of anticlinal and synclinal structures with prescribed depth dependent density. *Geophysical Prospecting*, 55, 571–587.
- Chakravarthi, V. and Sundararajan, N., 2008, TODGINV—A code for optimization of gravity anomalies due to anticlinal and synclinal structures with parabolic density contrast. *Computers & Geosciences*, 34, 955–966
- El-Kaliouby, H.M. and Al-Garni, M.A., 2009, Inversion of self-potential anomalies caused by 2D inclined sheets using neural networks. *J. Geophys. Eng.*, 6, 29–34.
- Eshaghzadeh, A. and Hajian, A.R., 2018, 2D inverse modeling of residual gravity anomalies from Simple geometric shapes using Modular Feed-forward Neural Network. *Annals of Geophysics*, 61, 1, SE115.
- Eslam, E., Salem, A. and Ushijima, K., 2001, Detection of cavities and tunnels from gravity data using a neural network. *Explor. Geophys.*, 32, 204-208.
- Hagan, M.T., Demuth, H.B. and Beale, M.H., 1996, *Neural Network Design*. PWS Publishing Company, Boston, Massachusetts.
- Heiland, C.A., 1968, *Geophysical Exploration*. 2nd ed. Hafner Publishing Co., New York.
- Huang, Z., Shimeld, J., Williamson, M. and Katsube, J., 1996, Permeability prediction with artificial neural network modeling in the venture gas field, offshore eastern Canada. *Geophysics*, 61, 422-436.
- Macias, C., Sen M.K. and Stoffa P.L., 2000, Artificial neural networks for parameter estimation in geophysics. *Geophysical Prospecting*, 48, 21-47.
- Osman, O., Muhittin, A.A. and Ucan O.N., 2006, A new approach for residual gravity anomaly profile interpretations: Forced Neural Network (FNN). *Ann. Geofis.*, 49, 6.
- Osman, O., Albora, A.M. and Ucan, O.U., 2007, Forward modeling with forced Neural networks for gravity anomaly profile. *Math. Geol.*, 39, 593-605.
- Pearson, W., Wiener, J. and Moll, R., 1990, Aeromagnetic structural interpretation using neural networks” A case study from the northern Denver-Julesberg Basin”, *Ann International Meeting, Soc. Expl. Geophysics*, Expanded abstract., 587-590.
- Rao, K.G.C. and Avasthi, D.N., 1973, Analysis of the Fourier spectrum of the gravity effect due to two-dimensional triangular prism. *Geophysical Prospecting*, 21, 526–542.
- Rao, B.S.R. and Murty, I.V.R., 1978, *Gravity and Magnetic Methods of Prospecting*. Arnold-Heinemann Publishers, New Delhi, India.
- Rojas, R., 1996, *Neural Networks: A Systematic Introduction*. Springer-Verlag, Berlin.
- Rummelhart, D.E., Hinton, G.E. and Williams, R.J., 1986, Learning internal representation by back propagating errors. *Nature*, 332, 533–536.
- Salem, A., Elawadi, E., Abdelaziz, A. and Ushijima, K., 2001, Imaging subsurface cavities from microgravity data using Hopfield neural network, *Proceeding of the 5th SEGJ International Symposium*, Toty, 199-205.